Barrier transmission for the one-dimensional nonlinear Schrödinger equation: Resonances and transmission profiles

K. Rapedius and H. J. Korsch*
Fachbereich Physik, Technische Universität Kaiserslautern, D-67653 Kaiserslautern, Germany
(Received 19 June 2007; revised manuscript received 13 February 2008; published 12 June 2008)

The stationary nonlinear Schrödinger equation (or Gross-Pitaevskii equation) for one-dimensional potential scattering is studied. The nonlinear transmission function shows a distorted profile, which differs from the Lorentzian one found in the linear case. This nonlinear profile function is analyzed and related to Siegert-type complex resonances. It is shown that the characteristic nonlinear profile function can be conveniently described in terms of skeleton functions depending on a few instructive parameters. These skeleton functions also determine the decay behavior of the underlying resonance state. Furthermore, we extend the Siegert method for calculating resonances, which provides a convenient recipe for calculating nonlinear resonances. Applications to a double Gaussian barrier and a square-well potential illustrate our analysis.

DOI: 10.1103/PhysRevA.77.063610 PACS number(s): 03.75.Lm, 03.65.−w, 03.75.Kk

I. INTRODUCTION

Transport properties of Bose-Einstein condensates (BECs) are of considerable current interest, both experimentally and theoretically. In particular, atom-chip experiments are well-suited to study the influence of interatomic interaction on transport properties of BECs in waveguides since various waveguide geometries can be realized by different methods [1–10].

A convenient theoretical approach is based on the Gross-Pitaevskii equation (GPE) or the nonlinear Schrödinger equation (NLSE),

$$i\hbar\frac{\partial\psi(\mathbf{x},t)}{\partial t}=\left(-\frac{\hbar^2}{2m}\nabla^2+V(\mathbf{x})+g|\psi(\mathbf{x},t)|^2\right)\psi(\mathbf{x},t), \quad (1)$$

which describes the dynamics in a mean-field approximation at low temperatures [11–14]. Another important application of the NLSE is the propagation of electromagnetic waves in nonlinear media (see, e.g., [15], Chap. 8). The ansatz $\psi(\mathbf{x},t)=\exp(-i\mu t/\hbar)\psi(\mathbf{x})$ reduces Eq. (1) to the corresponding time-independent NLSE,

$$\left(-\frac{\hbar^2}{2m}\nabla^2+V(\mathbf{x})+g|\psi(\mathbf{x})|^2\right)\psi(\mathbf{x})=\mu\psi(\mathbf{x}) \quad (2)$$

with the chemical potential μ.

Various interesting phenomena have been reported originating from the nonlinearity of Eq. (1), such as, for instance, a bistability of the barrier transmission probability [16–19]. A paradigmatic model in this context is the transmission through a one-dimensional rectangular barrier or across a square-well potential, one of the rare cases in which the one-dimensional NLSE

$$\frac{\hbar^2}{2m}\psi''+(\mu-V)\psi-g|\psi|^2\psi=0 \quad (3)$$

can be solved analytically [19–22]. As an example, Fig. 1 shows the nonlinear transmission coefficient $|T|^2$ as a function of the chemical potential for the square-well potential considered in [19], which is discussed in more detail in Sec. IV.

One observes a clearly structured behavior: the well-known Lorentz profiles determined by the complex-valued resonances for linear transmission are distorted. The curves bend to the right (to the left for attractive nonlinearity $g<0$) and are multivalued in certain regions. A time-dependent numerical analysis shows that the lowest branch of the transmission coefficient is populated if an initially empty waveguide is slowly filled with condensate with a fixed chemical potential μ [16,19], whereas the highest branch can be populated if the chemical potential is adiabatically increased during the propagation process, which is equivalent to applying an additional weak time-dependent potential [16]. These and related aspects are discussed in detail in [23].

It is the purpose of the present paper to analyze the functional form of the transmission profile of the resonance peaks characterized by $|T|^2=1$ for a general (symmetric) potential by relating them to Siegert-type complex-valued resonances. It is demonstrated that the nonlinear resonances can be conveniently described by two skeleton functions that can be easily computed and approximately fitted by a few parameters. In particular, we show that the line shape of the reso-

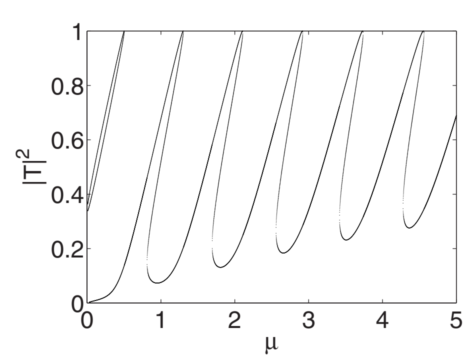

FIG. 1. (Units $\hbar=m=1$.) Transmission coefficient obtained from solving the stationary NLSE (3) for a square-well potential with $b=20$ and $V_0=-50$ for $g=+1$ (see Sec. IV B and [19]).

*korsch@physik.uni-kl.de

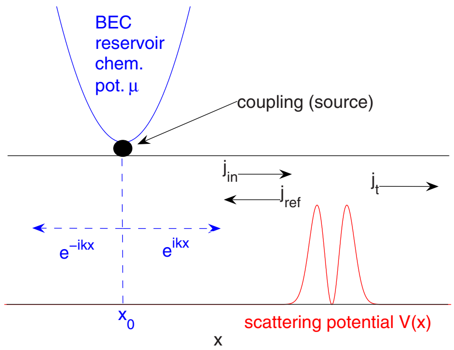

FIG. 2. (Color online) At x_0 condensate with chemical potential μ is injected into the waveguide from a reservoir. The reservoir emits a plane matter wave in both directions into the guide so that an incoming beam with current $j_{\rm in}$ is partially reflected (current $j_{\rm ref}$) and partially transmitted (current j_t) at the barrier potential $V(x)$.

nance peaks is determined by the decay behavior of the underlying metastable resonance state.

The paper is organized as follows. In Sec. II, we discuss the nonlinear transmission problem and develop a formula for the nonlinear Lorentz profiles that describes the transmission coefficient in the vicinity of a resonance in terms of skeleton functions. In Sec. III, we present a convenient recipe for calculating nonlinear resonances and skeleton curves by a Siegert method. The applicability of this technique to the nonlinear resonance theory of Sec. II is illustrated in Sec. IV for two example potentials. Two Appendixes present additional material, namely the continuation of solutions of the NLSE to complex chemical potentials in Appendix A, and, in Appendix B, the derivation of a useful formula for the decay coefficient for a symmetric finite range potential, denoted as the Siegert relation.

II. NONLINEAR LORENTZ PROFILE

A. The transmission problem

In the case of the NLSE, the superposition principle is not valid. Therefore, the definition of a transmission coefficient is nontrivial. Here we review and slightly extend an approach based on the time-dependent NLSE (see [16,19,23]). Following Paul *et al.* [23], we consider an experimental setup where matter waves from a large reservoir of condensed atoms at chemical potential μ are injected into a one-dimensional waveguide in which the condensate can propagate (see Fig. 2). In a time-dependent approach, the system is described by the NLSE,

$$i\hbar\dot{\psi}(x,t) = -\frac{\hbar^2}{2m}\psi''(x,t) + V(x)\psi(x,t) + g|\psi(x,t)|^2\psi(x,t) + f(t)\mathrm{e}^{-i\mu t/\hbar}\delta(x-x_0), \quad (4)$$

where the source term $f(t)\mathrm{e}^{-i\mu t/\hbar}\delta(x-x_0)$ located at $x=x_0$ emits monochromatic matter waves at chemical potential μ and thus simulates the coupling to a reservoir. The barrier potential $V(x)$ is assumed to be zero for $x\leq x_0$.

In the following, we assume a constant source strength $f(t)=f_0$ and look for stationary solutions $\psi(x,t)=\psi(x)\exp(-i\mu t/\hbar)$ of Eq. (5) arriving at

$$\mu\psi(x) = -\frac{\hbar^2}{2m}\psi''(x) + V(x)\psi(x) + g|\psi(x,t)|^2\psi(x,t) + f_0\delta(x-x_0). \quad (5)$$

Application of the integral operator

$$\lim_{\epsilon\to 0}\int_{x_0-\epsilon}^{x_0+\epsilon} dx \quad (6)$$

leads to

$$-\frac{\hbar^2}{2m}(\psi_+' - \psi_-')\Big|_{x_0} + f_0 = 0, \quad (7)$$

where we have introduced the notation

$$\psi(x) = \begin{cases} \psi_-(x), & x \leq x_0 \\ \psi_+(x), & x > x_0. \end{cases} \quad (8)$$

Since we have $V(x)=0$, $x\leq x_0$ and there is no incoming current from $x=-\infty$, the solution in the region $x\leq x_0$ is given by the plane wave $\psi_-(x)=\psi_-^0\exp(-ik_-x)$ with $k_- = \sqrt{2m(\mu-g|\psi_-^0|^2)}/\hbar$ and $\psi_-'(x)=-ik_-\psi_-(x)$. Inserting this into Eq. (7) leads to

$$f_0 = \frac{\hbar^2}{2m}(\psi_+' + ik_-\psi_-)\Big|_{x_0} \quad (9)$$

or, taking into account the continuity of the wave function $(\psi_+-\psi_-)|_{x_0}=0$ at $x=x_0$, to

$$f_0 = \frac{\hbar^2}{2m}(\psi_+' + ik_+\psi_+)\Big|_{x_0} \quad (10)$$

with $k_+=\sqrt{2m[\mu-g|\psi_+(x_0)|^2]}/\hbar$. Equation (10) relates the wave function ψ_+ in the region $x\geq x_0$ to the source strength f_0. In order to relate the source strength to the incoming condensate current, we consider the special case in which $V(x)=0$ everywhere, i.e., without a barrier. Then the wave function in the region $x\geq x_0$ is given by a plane wave $\psi_+(x)=A\exp[ik_A(x-x0)]$ with $k_A=\sqrt{2m(\mu-g|A|^2)}/\hbar$ and $\psi_+'(x)=-ik_A\psi_+(x)$. From the continuity of the wave function $\psi_-(x_0)=\psi_+(x_0)=A$, we get $k_-=k_+=k_A$, and together with Eq. (10) we obtain

$$f_0 = i\frac{\hbar^2}{m}k_A A. \quad (11)$$

For a given source strength f_0, Eq. (11) can have up to two different solutions for A. In the following, we only consider the solution corresponding to the limit of weak interaction. The incoming current emitted by the source is given by $j_{\rm in}=\frac{\hbar}{m}k_A|A|^2=|f_0||A|/\hbar$. Inserting Eq. (11) into Eq. (10), we obtain the relation

$$2ik_A A = (\psi_+' + ik_+\psi_+)|_{x_0} \quad (12)$$

connecting the condensate wave function with the incoming current. We define the transmission coefficient as

$$|T|^2 = \frac{j_t}{j_{\rm in}}, \tag{13}$$

where the current j_t transmitted through the barrier is obtained by evaluating the current operator

$$j_t = -\frac{i\hbar}{2m}(\psi_+^* \psi_+' - \psi_+ \psi_+'^*) \tag{14}$$

anywhere in the region $x \geq x_0$, and $j_{\rm in}$ is the current in absence of the barrier. In the noninteracting limit $g \to 0$, this definition coincides with the usual definition of the transmission coefficient known from the linear Schrödinger theory. It has the advantage of being also applicable in the time-dependent case.

In order to illuminate the dependence of the transmission coefficient on the position x_0 of the source term, we consider the transmission through a single δ barrier $V(x) = \lambda \delta(x)$ located at $x=0$ as a fixed output problem, i.e., we always have $\psi(x) = C \exp(ikx)$ for $x \geq 0$ with a fixed value of C. Since we are only interested in the influence of the nonlinearity in the upstream region $x \leq 0$, we set $g=0$ for $x>0$ so that $k = \sqrt{2m\mu}/\hbar$. If there is no reflection, the wave function in the upstream region $x \leq 0$ is given by a plane wave and the transmission coefficient is always equal to unity, independent of the position of the source. In the opposite limit of total reflection, the transmission coefficient is zero for any position of the source term. Thus the strongest position dependence can be expected for an intermediate transmittivity. For our study, we therefore choose the parameters $\lambda=2$, $\mu=2$, and $C=0.5$, which lead to a transmission of $|T|^2=0.5$ in the noninteracting ($g=0$) limit.

In the general case, the wave function $\psi(x)$ in the upstream region $x \leq 0$ is given by a Jacobi elliptic function with a period Δx (see, e.g., [19] and references therein). Thus the position dependence of the transmission coefficient inherits the same periodicity as we can see in the middle panel of Fig. 3, which shows the transmission coefficient $|T|^2$ in dependence on the position x_0 of the source term for a fixed nonlinearity of $g=0.1$. The amplitude of the oscillation increases with the interaction parameter g as shown in the upper panel of Fig. 3, where the maximum (solid red curve) and minimum (dashed blue) value of the transmission coefficient are plotted against g. For comparison, the dashed-dotted black curve shows the transmission according to an ansatz resulting from a thought experiment where the interaction parameter $g(x)$ is adiabatically ramped up from some position x_1 with $g(x_1)=0$ to its final value $g(x_1+L)=g_{\rm final}$ over some distance L. By relating the current in the region $x<x_1$, where $g(x)=0$ and thus the superposition principle is valid, to an adiabatically invariant quantity that is independent of the position x, the transmission coefficient can be expressed by the formula

$$|T|^2 = \left(1 + \frac{\hbar}{2\pi m j_t}\int_{\Delta x} [\partial_x |\psi(x)|]^2 dx\right)^{-1} \tag{15}$$

(see [23] for details), which requires integration over the spatial period Δx. It assumes a fixed incoming current $j_{\rm in}$ rather than a fixed source strength f_0 as the definition given in Eqs. (12)–(14). In the linear case ($g=0$), both definitions are equivalent but in the presence of interaction they differ due to the back-reaction of the effective interaction potential $g|\psi(x)|^2$ (see the lower panel of Fig. 3) on the source. One observes that the transmission according to Eq. (15) agrees reasonably well with the minimum value of the position-dependent transmission coefficient where the influence of the effective potential is small.

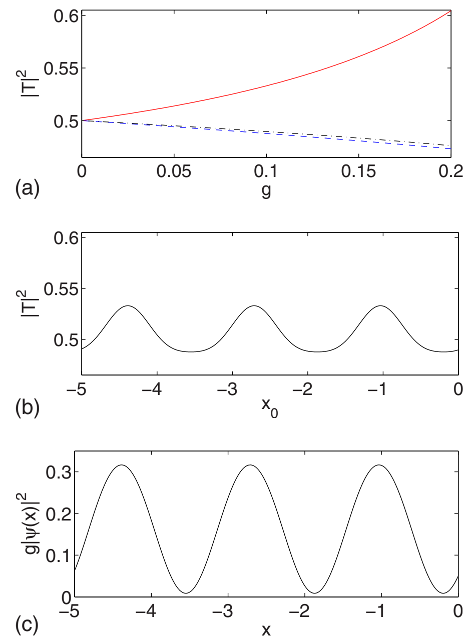

FIG. 3. (Color online) (Units $\hbar = m = 1$.) Upper panel: Maximum (solid red) and minimum value (dashed blue) of the transmission coefficient $|T|^2$ for different values of the interaction parameter g. Dashed-dotted black curve: transmission coefficient according to Eq. (15) for comparison. Middle panel: position dependence of the transmission coefficient for a fixed interaction strength $g=0.1$. Lower panel: Effective interaction potential $g|\psi(x)|^2$ for $g=0.1$.

In the vicinity of a resonance, the effective interaction potential $g|\psi(x)|^2$ outside the barrier is typically very small compared to the chemical potential so that the dependence on the source position is weak. Therefore, a good agreement between both definitions of the transmission coefficient can easily be achieved by an appropriate choice of the source position x_0 within one spatial period Δx (cf. Sec. IV A).

B. Resonance line shape

In the following, we will derive a formula for the transmission coefficient $|T|^2$ of a symmetric potential well $V(x) = V(-x)$ with the finite range a [i.e., $V(x)=0$ if $|x|>a$] in the vicinity of a resonance in dependence on the chemical potential μ of the incoming condensate current. Our approach is based on a generalization of Siegert's derivation of the dispersion formula for nuclear reactions, and we closely follow the arguments in [24]. An alternative ansatz makes use of the Feshbach formalism [23,25].

We consider the situation in which the condensate source is located at $x_0 = -a$. The solution in the downstream region $x>a$ is then given by a plane wave $\psi(x) = C\exp(ik_C x)$ with

$k_C = \sqrt{2m(\mu - g|C|^2)}/\hbar$ so that the transmitted current is given by $j_t = \frac{\hbar}{m} k_C |C|^2$. At $x=-a$, the wave function must satisfy Eq. (12) with $x_0=-a$.

Thus the scattering wave function ψ in the interval $[-a,a]$ is a solution of Eq. (3) with boundary conditions

$$\psi(a) = C e^{ik_C a}, \quad \psi'(a) = ik_C \psi(a), \tag{16}$$

$$2ik_A A = \psi'(-a) + ik\psi(-a), \tag{17}$$

where $k = \sqrt{2m[\mu - g|\psi(-a)|^2]}/\hbar$. The transmission coefficient given by $|T|^2 = j_t / j_{in} = (k_C/k_A)|C/A|^2$ depends on the chemical potential μ and, due to the nonlinear term in Eq. (3), also on the magnitude of the wave function. If the incoming amplitude A is kept fixed, this dependence can be conveniently described by the magnitude $|C|^2$ of the outgoing amplitude.

Now we consider C/A as a function of μ. From Eqs. (16) and (17), we obtain

$$\frac{C}{A} = \frac{2ik_A \psi(a) \exp[-i(k+k_C)a]}{ik\psi(-a) + \psi'(-a)}. \tag{18}$$

Singularities of Eq. (18) occur for certain complex chemical potentials W_{sk} where the denominator vanishes. These values of the chemical potential are defined by the eigenvalue problem

$$\frac{\hbar^2}{2m}\psi''_{sk} + (W_{sk} - V)\psi_{sk} - g|\psi_{sk}|^2\psi_{sk} = 0 \tag{19}$$

in $-a \le x \le a$ with the boundary conditions

$$\psi_{sk}(a) = C e^{ik_{sk}a}, \quad \psi'_{sk}(a) = ik_{sk}\psi_{sk}(a), \tag{20}$$

$$\psi_{sk}(-a) = C e^{i(k_{sk}a + i\delta)}, \quad \psi'_{sk}(-a) = -ik_{sk}\psi_{sk}(-a), \tag{21}$$

where $k_{sk} = \sqrt{2m(W_{sk} - g|C|^2)}/\hbar$ and δ is some real-valued phase. Because of the nonlinear term in Eq. (19), the complex energy $W_{sk} = \mu_{sk} - i\Gamma_{sk}/2$ with real μ_{sk} and Γ_{sk} depends explicitly on $|C|^2$. The problem concerning the continuation of the solution to the domain of complex chemical potentials is discussed in Appendix A. Motivated by the analogy to a driven nonlinear oscillator, we call the functions $\mu_{sk}(|C|^2)$ and $\Gamma_{sk}(|C|^2)$ *skeleton curves* and ψ_{sk} the *skeleton wave function*.

From Eq. (19) and its complex conjugate as well as the boundary conditions (20) and (21), we derive the useful formula

$$\frac{\hbar^2}{2m}|\psi_{sk}(a)|^2 = \frac{\Gamma_{sk}/2}{k_{sk} + k^*_{sk}} \int_{-a}^{a} |\psi_{sk}|^2 dx. \tag{22}$$

In order to obtain C/A in the vicinity of the singularity W_{sk}, we multiply Eq. (3) by ψ_{sk} and Eq. (19) by ψ and subtract these equations. By integrating the resulting equation

$$\frac{\hbar^2}{2m}(\psi''_{sk}\psi - \psi''\psi_{sk}) + (W_{sk} - \mu)\psi_{sk}\psi + g\psi_{sk}\psi(|\psi|^2 - |\psi_{sk}|^2) = 0 \tag{23}$$

from $x=-a$ to $x=+a$ and using the boundary conditions, we arrive at

$$\frac{\hbar^2}{2m}\{i\psi_{sk}(a)\psi(a)(k_{sk} - k_C) + \psi_{sk}(-a)[ik_{sk}\psi(-a) + \psi'(-a)]\} + g\int_{-a}^{a}\psi_{sk}\psi(|\psi|^2 - |\psi_{sk}|^2)dx + (W_{sk} - \mu)\int_{-a}^{a}\psi_{sk}\psi dx = 0. \tag{24}$$

Thus we can write the denominator of C/A in Eq. (18) as

$$\begin{aligned} ik\psi(-a) + \psi'(-a) = &-\frac{W_{sk} - \mu}{(\hbar^2/2m)\psi_{sk}(-a)}\int_{-a}^{a}\psi_{sk}\psi dx \\ &- \frac{2mg}{\hbar^2\psi_{sk}(-a)}\int_{-a}^{a}\psi_{sk}\psi(|\psi|^2 - |\psi_{sk}|^2)dx \\ &- i(k_{sk} - k_C)\frac{\psi_{sk}(a)\psi(a)}{\psi_{sk}(-a)} - i(k_{sk} - k) \\ &\times \psi(-a). \end{aligned} \tag{25}$$

Using

$$k_{sk} - k_C = \frac{2m}{\hbar^2}\frac{W_{sk} - \mu}{k_{sk} + k_C}, \tag{26}$$

$$k_{sk} - k = \frac{2m}{\hbar^2}\frac{W_{sk} - \mu - g[|C|^2 - |\psi(-a)|^2]}{k_{sk} + k}, \tag{27}$$

we obtain

$$\begin{aligned} ik\psi(-a) + \psi'(-a) = &-\frac{W_{sk} - \mu}{(\hbar^2/2m)\psi_{sk}(-a)}\int_{-a}^{a}\psi_{sk}\psi dx \\ &- \frac{2mg}{\hbar^2\psi_{sk}(-a)}\int_{-a}^{a}\psi_{sk}\psi(|\psi|^2 - |\psi_{sk}|^2)dx \\ &- i\frac{W_{sk} - \mu}{(\hbar^2/2m)\psi_{sk}(-a)}\frac{\psi_{sk}(a)\psi(a)}{k_{sk} + k_C} \\ &- i\frac{W_{sk} - \mu - g[|C|^2 - |\psi(-a)|^2]}{(\hbar^2/2m)\psi_{sk}(-a)} \\ &\times \frac{\psi_{sk}(-a)\psi(-a)}{k_{sk} + k}. \end{aligned} \tag{28}$$

Assuming that the eigenvalue W_{sk} is not degenerate, we have the following in the limit $\mu \to W_{sk}$: $\psi \to \psi_{sk}$, $|\psi(-a)|^2 \to |C|^2$, and $k, k_C \to k_{sk}$, so that

$$ik\psi(-a) + \psi'(-a) \to -\frac{W_{sk} - \mu}{(\hbar^2/2m)\psi_{sk}(-a)}\left(\int_{-a}^{a}\psi^2_{sk}dx + i\frac{\psi^2_{sk}(a) + \psi^2_{sk}(-a)}{2k_{sk}}\right). \tag{29}$$

For the numerator of C/A, we get $2ik_A\psi(a)\exp[-i(k+k_C)a] \to 2ik_A\psi_{sk}(a)\exp(-2ik_{sk}a)$. Thus C/A becomes

$$\frac{C}{A} = -\frac{\hbar^2/2m}{W_{sk} - \mu}\frac{2ik_A e^{-2ik_{sk}a}\psi_{sk}(a)\psi_{sk}(-a)}{\int_{-a}^{a}\psi^2_{sk}dx + i\frac{\psi^2_{sk}(a) + \psi^2_{sk}(-a)}{2k_{sk}}}. \tag{30}$$

For sufficiently small values of Γ_{sk}, we can multiply ψ_{sk} by a suitable constant ζ of magnitude 1 that makes $\zeta\psi_{sk}$ real (up to terms of order Γ_{sk}) in the regions of slowly varying phase, which give the main contribution to the integral $\int_{-a}^{a}|\psi_{sk}|^2 dx$. In this limit, we can thus use the approximation

$$\int_{-a}^{a} \zeta^2 \psi_{sk}^2 dx \approx \int_{-a}^{a} |\psi_{sk}|^2 dx. \tag{31}$$

We furthermore define the phase factor δ_{sk} by $\zeta\psi_{sk}(a) = |\psi_{sk}(a)|\exp(ik_{sk}a + i\delta_{sk}/2)$. Using these definitions and $\psi_{sk}(-a) = \psi_{sk}(+a)\exp(i\delta)$, Eq. (30) can be written as

$$\frac{C}{A} = -\frac{\hbar^2/2m}{W_{sk}-\mu} \frac{2ik_A \exp(i\delta_{sk}+i\delta)|\psi_{sk}(a)|^2}{\int_{-a}^{a}|\psi_{sk}|^2 dx + i|\psi_{sk}(a)|^2 \frac{\exp(2ik_{sk}a+i\delta_{sk})[1+\exp(i\delta)]}{2k_{sk}}} \tag{32}$$

or, using Eq. (22),

$$\frac{C}{A} = -e^{i\delta_{sk}+i\delta} \frac{\Gamma_{sk}/2}{W_{sk}-\mu} \frac{2ik_A}{k_{sk}+k_{sk}^* + i\Gamma_{sk}\frac{2m\exp(2ik_{sk}a+i\delta_{sk})[1+\exp(i\delta)]}{\hbar^2 k_{sk}}}. \tag{33}$$

As Γ_{sk} tends to zero, k_{sk} becomes real and the last term in the denominator of Eq. (33) is negligible, so that we have in this limit

$$\frac{C}{A} = e^{i\delta_{sk}+i\delta} \frac{k_A}{k_{sk}} \frac{i\Gamma_{sk}/2}{\mu - \mu_{sk} + i\Gamma_{sk}/2}. \tag{34}$$

Thus the transmission coefficient in the vicinity of a resonance is given by

$$|T|^2 = \frac{k_C}{k_A}\left|\frac{C}{A}\right|^2 = \frac{k_A}{k_{sk}} \frac{\Gamma_{sk}^2/4}{(\mu-\mu_{sk})^2 + \Gamma_{sk}^2/4} \tag{35}$$

with $k_{sk} \approx k_C$. This result formally resembles the Lorentz or Breit-Wigner form that occurs in the respective linear theory. However, the chemical potential μ_{sk} and the width Γ_{sk} depend implicitly on $|T|^2$. This dependence disappears in the linear limit $g \to 0$ and we recover the usual Lorentz profile. Equation (35) can be inverted to the form

$$\mu_{\pm} = \mu_{sk} \pm \frac{\Gamma_{sk}}{2}\sqrt{\frac{k_A}{k_{sk}|T|^2} - 1}, \tag{36}$$

i.e., the skeleton chemical potential is the average of the two branches $\mu_{\pm}$ at fixed $|T|^2$ and the skeleton Γ_{sk} the ($|T|$-weighted) width

$$\Gamma_{sk} = [\mu_+(|T|) - \mu_-(|T|)]\sqrt{\frac{|T|^2}{(k_A/k_{sk}) - |T|^2}}. \tag{37}$$

Figure 5 shows a typical nonlinear Lorentz curve of the type (35) for the case of a repulsive nonlinearity. The skeleton curve μ_{sk}, indicated by the dashed line, appears as a kind of backbone structure of the nonlinear Lorentz profile, justifying its name, which is taken from the theory of classical driven nonlinear oscillators [26] where resonance curves similar to Eq. (35) occur.

The skeleton curves μ_{sk} and Γ_{sk} can either be parametrized in terms of the amplitude $|C|^2$ or in terms of the number of particles $N = \int_{-b}^{b}|\psi_{sk}(x)|^2 dx$ inside the potential well. It was shown [27,28] that in an adiabatic approximation, the decay behavior of a resonance state is determined by the imaginary part $\Gamma_{sk}[N(t)]$ of the instantaneous chemical potential via

$$\partial_t N(t) = -\frac{\Gamma_{sk}[N(t)]}{\hbar} N(t). \tag{38}$$

Thus there is a close connection between the transmission line shape and the decay behavior of the corresponding resonance state as it is known for the linear limit $g=0$, where the decay coefficient is constant and the line shape is Lorentzian.

III. CALCULATING SKELETON CURVES

As shown in Sec. II, the skeleton curves $\mu_{sk}(|C|^2)$ and $\Gamma_{sk}(|C|^2)$ are obtained by solving the NLSE (19) with the Siegert boundary conditions (20) and (21). It has been shown that the use of Siegert boundary conditions is equivalent to a complex rotation of the coordinates [29]. Different procedures based on this principle, e.g., direct complex scaling or complex absorbing potentials, have been successfully applied to resonance states of the NLSE [27,30,31]. Here we present an alternative method that is numerically cheap, easy to implement, and, though not quite as accurate as the complex scaling procedures, provides a convenient basis for approximations.

This method, which we call the Siegert method, is based on neglecting the imaginary part $-\Gamma_{sk}/2$ of the chemical potential and thus having only real values of $k_{sk} = \sqrt{2m(\mu_{sk} - g|C|^2)}/\hbar$, which is justified for not too large values of Γ_{sk}. Since the boundary conditions (20) and (21) can no longer be satisfied simultaneously for real values of k_{sk}, we replace the boundary conditions (21) by the less restricting condition

$$\left.\frac{d}{dx}|\psi_{sk}|^2\right|_{x=0} = 0, \tag{39}$$

which preserves the symmetry $|\psi_{sk}(-x)|^2 = |\psi_{sk}(x)|^2$ of the skeleton wave functions. This is equivalent to calculating the wave function for which the transmission coefficient assumes a maximum. The new boundary value problem given by Eqs. (19), (20), and (39) is solved using a shooting procedure where the NLSE (19) is integrated from $x=+a$ to $x=0$ using a Runge-Kutta solver with starting conditions (20) at $x=a$ for a fixed value of C. By means of a bisection method, μ_{sk} is adapted until the condition (39) is satisfied. The imaginary part of the chemical potential can then be estimated by the Siegert relation

$$\Gamma_{sk} = \frac{\hbar^2 k_{sk}|C|^2}{m\int_0^b |\psi_{sk}(x)|^2 dx}, \tag{40}$$

where $\pm b$ are the positions of the maxima of the symmetric trapping potential (see Appendix B).

TABLE I. Chemical potential and decay rates for the lowest quasibound state, calculated with the Siegert method (S), complex scaling (CS), and complex absorbing potentials (CAP) (units $\hbar = m = 1$).

g	μ_{S}	μ_{CS}	μ_{CAP}	$\Gamma_{\mathrm{S}}/2$	$\Gamma_{\mathrm{CS}}/2$	$\Gamma_{\mathrm{CAP}}/2$
0	0.4601	0.4601	0.4602	9.63e-7	9.35e-7	9.62e-7
1	0.7954	0.7954	0.7954	1.81e-5	1.82e-5	1.80e-5
2	1.0772	1.0765	1.0772	1.56e-4	1.55e-4	1.56e-4
3	1.3192	1.3190	1.3192	8.11e-4	8.05e-4	8.05e-4
4	1.5317	1.5315	1.5312	2.79e-3	2.76e-3	2.75e-3
5	1.7247	1.7236	1.7231	6.78e-3	6.65e-3	6.63e-3
6	1.9070	1.9043	1.9035	1.27e-2	1.24e-2	1.23e-2

Before we use our simple method to compute skeleton curves in Sec. IV, we demonstrate its validity for the lowest resonance state of the standard test potential,

$$V(x) = \frac{x^2}{2}\exp(-\alpha x^2) \tag{41}$$

with $\alpha = 0.1$ so that the position of the potential maxima is given by $b \approx 3.16$ using units where $\hbar = 1$ and $m = 1$ as we do for all numerical calculations in this paper. We choose $a = 30$ to be sufficiently large to ensure that the approximation $V(x) \approx 0$ for $|x| > a$ is valid and thus the resonance wave function $\psi_{\mathrm{sk}}(x)$ is well approximated by a plane wave in the area $x > a$. The amplitude C is chosen such that the wave function is normalized in the region $|x| \le b$, i.e., $\int_{-b}^{b} |\psi_{\mathrm{sk}}(x)|^2 dx = 1$. Note that because of the nonlinearity, ψ_{sk} is not proportional to C.

In Table I, we compare our results for the lowest resonance of the potential (41) with the results of direct complex scaling and the complex absorbing potential method [27]. The agreement between the different methods is very good, especially if the interaction constant g is small, which is also the case within our calculations of skeleton curves in the following section. Apart from being numerically cheap and easy to implement, the Siegert method proposed here can provide analytical expressions for μ_{sk} and Γ_{sk} if the potential in consideration is simple enough (see Sec. IV B).

The Siegert method can be generalized to resonances of asymmetric barrier potentials where the matter wave is localized between two maxima at $x = -c < 0$ and $x = b > 0$ with $|b|, |c| < a$, but then the situation is more involved because the symmetry condition (39) no longer applies. Instead one can again consider the problem of transmission through the barrier and calculate the states ψ_{asym} and the corresponding real chemical potentials μ_{asym} that maximize the transmission coefficient [see the remark following Eq. (39)]. The relation (40) for the decay coefficient is generalized to

$$\Gamma_{\mathrm{asym}} = \frac{\hbar^2 k_{+a} |\psi_{\mathrm{asym}}(a)|^2 + \hbar^2 k_{-a} |\psi_{\mathrm{asym}}(-a)|^2}{m \int_{-c}^{b} |\psi_{\mathrm{asym}}(x)|^2 dx}, \tag{42}$$

where $k_{\pm a} = \sqrt{2m[\mu_{\mathrm{asym}} - g|\psi(\pm a)|^2]}/\hbar$.

IV. APPLICATIONS

In the preceding section, we presented a convenient recipe for calculating nonlinear resonances and skeleton curves by a Siegert method. In this section, we will illustrate the applicability of this technique to the nonlinear resonance theory of Sec. II for two model potentials that illuminate special features of the transmission problem, namely a double-Gaussian barrier with full nonlinearity on the whole axis and a square well with vanishing nonlinearity outside the well. The approximate resonance results are compared with exact numerical computations. Finally, the decay behavior as a function of time is briefly discussed, again illustrated by the nonlinear square well.

To this end, we calculate the skeleton curves μ_{sk} and Γ_{sk}, which can either be parametrized in terms of the amplitude $|C|^2$ or in terms of the mean number of particles $N = \int_{-b}^{b} |\psi_{\mathrm{sk}}(x)|^2 dx$ inside the potential well, by means of the Siegert method presented in the preceding section. Furthermore, we show that these skeleton curves are conveniently approximated by polynomials depending on a few instructive parameters.

A. Example 1: The double-Gaussian barrier

To demonstrate the validity of our model (35), we apply it to the potential

$$V(x) = V_0\{\exp[-(x+b)^2/\alpha^2] + \exp[-(x-b)^2/\alpha^2]\} \tag{43}$$

for $|x| \le a$ and $V(x) = 0$ for $|x| > a$ with the parameters $V_0 = 1$, $b = 14.7/2$, $\alpha = b/5$, $a = 30$, and a nonlinearity of $g = 0.005$. The mean number of particles $N = \int_{-b}^{b} |\psi_{\mathrm{sk}}(x)|^2 dx$ inside the potential well is calculated between the maxima $x = \pm b$ of the potential (43); the source term shall be located at $x_0 = -a$. For the given parameters, the dependence of the transmission coefficient on the position of the source term is negligible (see Sec. II A). In [16], the transmission coefficient of this potential in dependence on μ is calculated for the case of an initially empty waveguide. The incoming amplitude $|A|^2$ is connected with the incident current j_{in} (i.e., the current in the absence of the barrier) via $j_{\mathrm{in}} = |A|^2 \sqrt{2(\mu - g|A|^2)}/m$. In the following, we will assume $|A|^2 = 1$ in all numerical calculations.

Using the method described in Sec. III, we numerically calculate the skeleton curves $\mu_{\mathrm{sk}}(|C|^2)$, $\Gamma_{\mathrm{sk}}(|C|^2)$ with $|C|^2$

$\leq |A|^2$. For $|C|^2 = |A|^2$, we have $|T|^2 = 1$ (see Sec. II). We call the quantities $\mu_R \equiv \mu_{\mathrm{sk}}(|C|^2 = |A|^2)$, $\Gamma_R \equiv \Gamma_{\mathrm{sk}}(|C|^2 = |A|^2)$, and $\psi_R(x) \equiv \psi_{\mathrm{sk}}(x; |C|^2 = |A|^2)$ the resonance chemical potential, resonance width, and resonance wave function, respectively. In the limit $|C|^2 \to 0$, the influence of the nonlinear term in the NLSE (19) can be neglected so that $\mu_{\mathrm{sk}}(|C|^2 \to 0) = \mu_n$ and $\Gamma_{\mathrm{sk}}(|C|^2 \to 0) = \Gamma_n$, where μ_n and Γ_n are the respective quantities of the linear problem with $g=0$.

Now we will show that over a wide range of parameters, the skeleton curves $\mu_{\mathrm{sk}}(N)$ and $\Gamma_{\mathrm{sk}}(N)$ are well approximated by simple elementary functions, and that the five quantities μ_n, Γ_n, μ_R, Γ_R, and $|A|^2$ provide all the necessary information.

Since the shift in the chemical potential is caused by the term $g|\psi_{\mathrm{sk}}|^2$ in the NLSE (19), we assume this shift to be approximately proportional to the number of particles inside the potential well, that is,

$$\mu_{\mathrm{sk}}(N) = \mu_n + \frac{\mu_R - \mu_n}{N_R} N, \tag{44}$$

where $N_R = \int_{-b}^{b} |\psi_R(x)|^2 dx$ is the norm inside the well in the case of resonance. Next we represent the amplitude $|C|^2 = |\psi(a)|^2$ as a function of N by a Taylor series that we truncate after the quadratic term,

$$|C|^2 \approx |T|^2 |A|^2 \approx \chi_1 N + \chi_2 N^2. \tag{45}$$

If there are no particles ($N=0$), the transmitted amplitude $|C|^2$ is zero so that there is no constant term in Eq. (45). Inserting Eqs. (44) and (45) into Eq. (40), we obtain

$$\Gamma_{\mathrm{sk}}(N) = \frac{2\hbar^2 k_{\mathrm{sk}} |C|^2}{N} \approx \frac{2\sqrt{2}\hbar}{\sqrt{m}} \sqrt{\mu_{\mathrm{sk}}(N) - g(\chi_1 N + \chi_2 N^2)}(\chi_1 + \chi_2 N). \tag{46}$$

From Eq. (46), we obtain

$$\Gamma_{\mathrm{sk}}(N=0) = \Gamma_n = 2\sqrt{2}\hbar\sqrt{\mu_n/m}\,\chi_1, \tag{47}$$

$$N_R = 2\hbar\sqrt{2}\sqrt{\mu_R - g|A|^2}|A|^2/(\sqrt{m}\Gamma_R), \tag{48}$$

so that the coefficients χ_1 and χ_2 are given by $\chi_1 = \Gamma_n\sqrt{m}/(2\hbar\sqrt{2\mu_n})$ and $\chi_2 = |A|^2/N_R^2 - \chi_1/N_R$. Inverting Eq. (45) leads to $N_\pm = -\chi_1/(2\chi_2) \pm \sqrt{\chi_1^2/(4\chi_2^2) + |C|^2/\chi_2}$. Thus we can compute μ_{sk} and Γ_{sk} as a function of $|T|^2$.

It is often useful to approximate Eq. (46) by a second-order Taylor polynomial

$$\Gamma_{\mathrm{sk}} = \Gamma_n(1 + \eta_1 N + \eta_2 N^2), \tag{49}$$

where $\eta_1 = \chi_2/\chi_1 + (\mu_R - \mu_n)/(2\mu_n N_R) - g\chi_1/\mu_n$ and $\eta_2 = \chi_2(\mu_R - \mu_n)/(2\mu_n N_R \chi_1) - g\chi_1/\mu_n - [(\mu_R - \mu_n)/(\mu_n N_R) - g\chi_1/\mu_n]^2$.

Figure 4 reveals an excellent agreement between the numerically calculated skeleton curves and the approximation described by Eqs. (44)–(48).

Figure 5 compares a peak of the transmission coefficient with the resonance model (35). While the qualitative features such as the bending of the curve are well reproduced, the resonance model (35) slightly overestimates the width of the resonance curve.

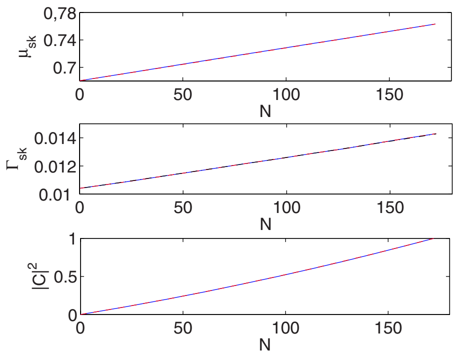

FIG. 4. (Color online) (Units $\hbar = m = 1$.) The numerically calculated curves $\mu_{\mathrm{sk}}(N)$, $\Gamma_{\mathrm{sk}}(N)$, and $|C|^2(N)$ (solid blue) and the approximation described by Eqs. (44)–(48) (dashed red) for the potential (43) as well as the Taylor approximation (49) (dashed-dotted black curve) are almost indistinguishable on the scale of drawing.

B. Example 2: The square well

For illustrative purposes, we now apply the result (35) to a simple analytically solvable toy model system that has a similar transmission behavior to the double-Gaussian barrier considered in the preceding section. In addition, it shows resonance peaks originating from the bound states of the corresponding linear ($g=0$) system that have been destabilized due to repulsive ($g>0$) interaction and have thus undergone a transition from bound to resonance state [19]. We consider the finite square-well potential with vanishing interaction outside the potential well, where the wave function $\psi(x)$ must satisfy

$$\left(-\frac{\hbar^2}{2m}\frac{d^2}{dx^2} - \mu\right)\psi(x) = 0, \quad |x| > b > 0 \tag{50}$$

and

$$\left(-\frac{\hbar^2}{2m}\frac{d^2}{dx^2} + g|\psi(x)|^2 + V_0 - \mu\right)\psi(x) = 0, \quad |x| \leq b \tag{51}$$

with $V_0 < 0$. The source term can be located at an arbitrary position $x_0 < -b$ since there is no interaction in this region so that the results do not depend on the position of the source

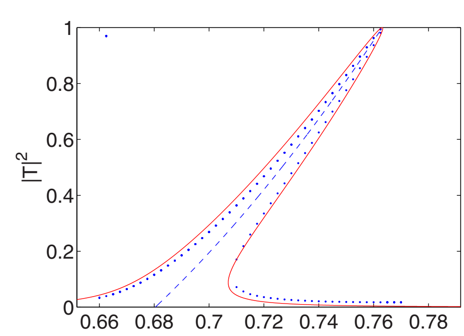

FIG. 5. (Color online) (Units $\hbar = m = 1$.) Comparison between the nonlinear Lorentz curve (35) (solid red curve) and the transmission coefficient obtained from solving the stationary NLSE (dotted blue curve) for the double-Gaussian potential (43). Dashed blue: skeleton curve $\mu_{\mathrm{sk}}(|T|^2)$.

term (see Sec. II A). This model with vanishing interaction outside the potential well was introduced in [19] in order to discuss the scattering process in terms of ingoing and outgoing waves and thus enabling an analytical treatment. In the context of nonlinear wave transmission, this assumption is widely used (see, e.g., [32]. and references therein). In principle, the interaction outside the potential well can be eliminated by means of a magnetic Feshbach resonance (see, e.g., [33]) or by a larger transversal extension $a_\perp$ of the waveguide in this region since the effective one-dimensional interaction strength is proportional to $1/a_\perp^2$ (see, e.g., [11]). Alternatively, instead of neglecting the interaction outside the potential well, one might add additional repulsive barriers at $x=\pm b$ without affecting much the qualitative behavior of the system with the disadvantage of making the analytical treatment more complicated.

In [19], the transmission coefficient is calculated analytically and it is shown that the respective states satisfying the NLSE (51) and (50) with the boundary conditions (20) and (39) (skeleton states) have the chemical potential

$$\mu_{\rm sk} = V_0 + \frac{3}{2}g|C|^2 + \frac{\hbar^2 K^2(p) n^2}{2mb^2}\begin{cases} 1+p \\ 1-2p, \end{cases} \tag{52}$$

where n is an integer number and $K(p)$ is the complete elliptic integral of the first kind (see e.g., [34]). The upper and lower alternatives correspond to $g|C|^2(V_0+g|C|^2)\geq 0$ and $0 \leq g|C|^2 \leq |V_0|$, respectively. The parameter $0\leq p\leq 1$ is determined by

$$g|A|^2(V_0+g|C|^2)\frac{2m^2b^4}{\hbar^4 n^4} = K^4(p)\begin{cases} p \\ p(p-1) \end{cases} \tag{53}$$

and the norm of the wave function inside the well reads

$$N = 2b|C|^2 + \frac{2\hbar^2 K(p) n^2}{gmb}\begin{cases} K(p)-E(p) \\ (1-p)K(p)-E(p). \end{cases} \tag{54}$$

Since $g=0$ in the region $|x|>b$, we have $k_{\rm sk}=\sqrt{2m\mu_{\rm sk}}/\hbar$ so that the decay width is given by

$$\Gamma_{\rm sk} = \frac{2\hbar\sqrt{2\mu_R}|C|^2}{\sqrt{m}N}, \tag{55}$$

where $\mu_{\rm sk}$ and N are given in Eqs. (52) and (54). As in Sec. IV A, the skeleton curves can be approximated by a Taylor polynomial. Applying our model to resonances of the square-well potential (50) and (51), it turns out that it is sufficient to truncate the Taylor polynomials in Eqs. (45) and (49) after the linear term. This leads to $N/N_R=|T|^2$ and thus

$$\mu_{\rm sk} = \mu_n + (\mu_R - \mu_n)|T|^2, \tag{56}$$

$$\Gamma_{\rm sk} = \Gamma_n + (\Gamma_R - \Gamma_n)|T|^2. \tag{57}$$

Figures 6 and 7 show the transmission probability $|T|^2(\mu)$ in the vicinity of a resonance, the exact solution, and the resonance approximation introduced in Sec. III for a deep square well with $V_0=-50$ and $b=20$. For both repulsive and attractive interaction, where the curves bend to the right or left, respectively, a good agreement between the nonlinear Lorentz curve (35) in a first-order approximation (56) and (57) and the respective resonance peak (see [19]) is observed. In particular, Fig. 7 shows that the nonlinear Lorentz curve (35) is also able to describe the unusually shaped peaks surrounding resonances that correspond to bound states in the linear limit $g\to 0$ (see [19]). The deviations are due to the fact that only a single resonance is included in the present approximation.

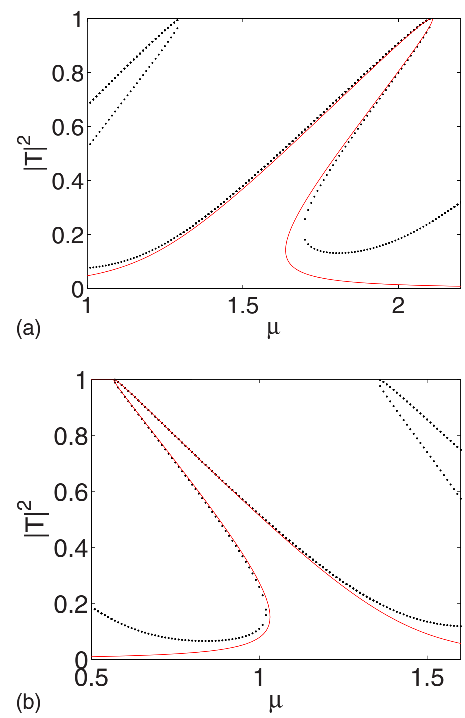

FIG. 6. (Color online) (Units $\hbar=m=1$.) Nonlinear Lorentz curve (35) (solid red curve) and transmission coefficient obtained from solving the stationary NLSE (dotted black curve) for a square-well potential with $b=20$, $V_0=-50$ for the resonance with quantum number $n=129$ for $g=+1$ (upper panel) and $g=-1$ (lower panel).

C. Decay behavior

As discussed in Sec. II, the decay behavior of the resonance state is described by

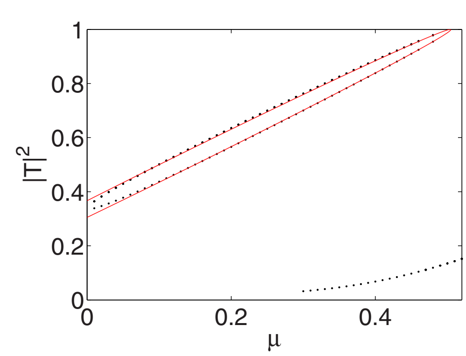

FIG. 7. (Color online) (Units $\hbar=m=1$.) Nonlinear Lorentz curve (35) (solid red curve) and transmission coefficient obtained from solving the stationary NLSE (dotted black curve) for a square-well potential with $b=20$, $V_0=-50$ for the resonance with quantum number $n=127$, which had been a bound state in the linear case $g=0$, for $g=+1$.

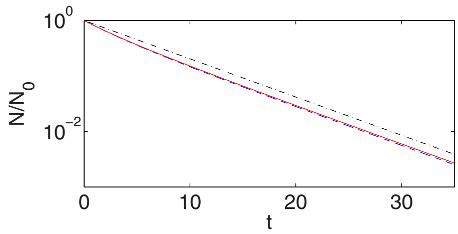

FIG. 8. (Color online) (Units $\hbar=m=1$.) Decay according to formula (61) (solid red line), the numerical solution of Eq. (58) (dashed blue line), and the linear decay behavior (dashed-dotted black line) for a potential well with parameters $b=20$, $V_0=-50$, and $g=+2$.

$$\partial_t N = -\frac{\Gamma_{\rm sk}(N)}{\hbar} N. \tag{58}$$

For the simple situation in which the skeleton curves are approximately linear in $|T|^2$, as in Eqs. (56) and (57), an analytical expression for the time dependence can be derived. With $\Gamma_{\rm sk}(N)=\Gamma_n+(\Gamma_R-\Gamma_n)(N/N_R)$, we obtain

$$\hbar\partial_t \frac{N}{N_R} = -\Gamma_n\frac{N}{N_R} - (\Gamma_R-\Gamma_n)\left(\frac{N}{N_R}\right)^2. \tag{59}$$

Separation of variables yields

$$-\frac{\hbar dy}{\Gamma_n y + (\Gamma_R-\Gamma_n)y^2} = dt \tag{60}$$

with $y=N/N_R$. This can be integrated to give

$$N(t) = \frac{\Gamma_n N_R}{\Gamma_R(e^{\Gamma_n(t-t_0)/\hbar}-1)+\Gamma_n}. \tag{61}$$

In the limit $g\to 0$, this reduces to the linear decay behavior $N(t)=N_R\exp[-\Gamma_n(t-t_0)/\hbar]$. In the limit of long times $t \gg t_0$, the system shows a linear decay $N(t) \to (\Gamma_n/\Gamma_R)N_R\exp[-\Gamma_n(t-t_0)/\hbar]\sim\exp[-\Gamma_n(t-t_0)/\hbar]$ as well.

As an example, Fig. 8 shows the decay according to formula (61) for the potential-well system (see example 2 above) in comparison with the numerical solution of Eq. (58) and the linear decay in a semilogarithmic plot. Formula (61) agrees well with the numerical solution of Eq. (58). In the limit of long times, both curves are parallel to the linear decay curve so that the system adopts a linear decay behavior as predicted above.

V. CONCLUSION

We have presented an analysis of the nonlinear resonances found for transmission of a BEC through a one-dimensional potential barrier in a mean-field GPE description. The Siegert method for determination of resonances is generalized to the nonlinear case providing a convenient recipe for the computation of nonlinear resonances.

Based on this Siegert method, we developed a formula for the nonlinear Lorentz profiles that can be described in terms of skeleton functions depending on a few instructive parameters. The skeleton curves also determine the decay behavior of the underlying resonance state thus relating the transmission line shape to the resonance lifetime.

Applications to a double-Gaussian barrier and a square-well potential illustrate and support our analysis. Finally, for a simple model an analytical expression for the decay behavior could be derived. We are therefore hopeful that the theoretical ideas presented may be useful in future work on nonlinear resonances.

ACKNOWLEDGMENTS

Support from the Deutsche Forschungsgemeinschaft via the Graduiertenkolleg ”Nichtlineare Optik und Ultrakurzzeitphysik” is gratefully acknowledged. We also thank Tobias Paul, Peter Schlagheck, and Dirk Witthaut for valuable discussions.

APPENDIX A: ANALYTICAL CONTINUATION

Since the NLSE

$$-\frac{\hbar^2}{2m}\psi''(x) + V(x)\psi(x) + g|\psi(x)|^2\psi(x) = \mu\psi(x) \tag{A1}$$

explicitly contains the squared magnitude $|\psi(x)|^2$ of the wave function, it is not analytical and therefore the analytical continuation of its solutions for complex values of μ is nontrivial. Following the arguments given in [35], we decompose the solution of the stationary GPE as $\psi(x)=X(x)+iY(x)$ with real functions $X(x)$ and $Y(x)$. From the real and imaginary part of Eq. (A1), we get a system of two equations,

$$-\frac{\hbar^2}{2m}X''(x) + V(x)X(x) + g[X^2(x)+Y^2(x)]X(x) = \mu X(x), \tag{A2}$$

$$-\frac{\hbar^2}{2m}Y''(x) + V(x)Y(x) + g[X^2(x)+Y^2(x)]Y(x) = \mu Y(x), \tag{A3}$$

which are analytical. The solutions of this system of equations, therefore, have a straightforward continuation into the domain of complex chemical potentials. As an example, we consider the plane-wave solution of the free $[V(x)=0]$ GPE with $\psi(x)=C\exp(ik_C x)$, $k_C=\sqrt{2m(\mu-g|C|^2)}/\hbar$, and $C=|C|\exp(i\theta)$. One can easily verify that its decomposition $X(x)=|C|\cos(k_C x+\theta)$, $Y(x)=|C|\sin(k_C x+\theta)$ satisfies the system (A2) and (A3) for all complex values of μ.

APPENDIX B: THE SIEGERT RELATION

Derivation. In the following, we will derive a formula for the decay coefficient of a resonance state of an arbitrary symmetric finite range potential. For the sake of generality and for future applications, we consider the cases of one, two, and three dimensions simultaneously. For now, we only consider resonances of the linear Schrödinger equation [Eq. (1)

with $g=0$]. The applicability to the nonlinear case is discussed separately further below.

Any solution $\psi(\mathbf{x},t)=\sqrt{\rho(\mathbf{x},t)}\exp[i\phi(\mathbf{x},t)]$ of the Schrödinger Eq. (1) with real functions $\phi(\mathbf{x},t)$ and $\rho(\mathbf{x},t)>0$ satisfies the continuity equation

$$\partial_t\rho+\mathrm{div}\mathbf{j}=0, \tag{B1}$$

where

$$\mathbf{j}=\frac{\hbar}{m}\rho\nabla\phi. \tag{B2}$$

Application of the Gauss theorem for vector fields leads to

$$\partial_t N=-\int_A \mathbf{j}\cdot d\mathbf{A}, \tag{B3}$$

where

$$N=\int_{\mathcal{V}}\rho(\mathbf{x},t)d^D\mathbf{x} \tag{B4}$$

is the norm of the wave function within a D-dimensional volume $\mathcal{V}$ and $\mathbf{A}=\partial(\mathcal{V})$ is the directed surface of $\mathcal{V}$. If the wave function is trapped inside the volume $\mathcal{V}$, the decay coefficient can be defined by the relation

$$\partial_t N=-\frac{\Gamma}{\hbar}N. \tag{B5}$$

Together with Eqs. (B3) and (B4), this leads to

$$\Gamma=-\hbar\frac{\partial_t N}{N}=\hbar\frac{\int \mathbf{j}\cdot d\mathbf{A}}{\int_{\mathcal{V}}\rho(\mathbf{x},t)d^D\mathbf{x}}. \tag{B6}$$

Now we consider a radially symmetric potential $V(\mathbf{x})=V(r)$ with finite range a, i.e., $V(r)=0$ if $r>a$, where $r=|\mathbf{x}|$. We assume the potential $V(r)$ to have a single maximum located at $b\leq a$. Assuming that the wave function varies slowly in time, we replace the time-dependent wave function $\psi(\mathbf{x},\mathbf{t})$ by the adiabatic resonance state $\psi(\mathbf{x})$ of the stationary Schrödinger equation [Eq. (2) with $g=0$]. Due to symmetry, the wave function in the area $r\leq a$ can be written in polar coordinates as

$$\psi(\mathbf{x})=R(r)Y(\Omega)\exp[i\phi_r(r)+i\phi_\Omega(\Omega)],\quad r\leq a, \tag{B7}$$

with real functions $R(r)$ and $Y(\Omega)$, where Ω stands for the angle variables. The resonance wave functions of such a potential are obtained by applying purely outgoing (Siegert) boundary conditions,

$$\psi(\mathbf{x})=R(a)\left(\frac{a}{r}\right)^{(D-1)/2}Y(\Omega)\exp[ik(r-a)+i\phi_r(a)+i\phi_\Omega(\Omega)],\quad r\geq a, \tag{B8}$$

where $k=\mathrm{Re}(\sqrt{2m\mu}/\hbar)$. For narrow resonances where $\Gamma/2=-\mathrm{Im}(\mu)$ is small compared to $\epsilon=\mathrm{Re}(\mu)$, we can make the approximation $k\approx\sqrt{2m\,\mathrm{Re}(\mu)}/\hbar$. For $D=1,3$, Eq. (B8) is an exact solution; for $D=2$, it only holds in the limit $a\to\infty$ (see below). This ansatz makes the wave function continuous at $r=a$. The continuity of the derivative implies the conditions

$$R'(a)=\frac{1-D}{2a}R(a),\quad \phi_r'(a)=k, \tag{B9}$$

where the prime denotes the partial derivative with respect to r.

The resonance wave function shall be trapped in the region $0\leq r\leq b$. Thus the volume $\mathcal{V}$ is a D-dimensional sphere with radius b so that $d^D\mathbf{x}=r^{D-1}drd\Omega$ and $d\mathbf{A}=\mathbf{e}_r b^{D-1}d\Omega$, where $\mathbf{e}_r$ is a unit vector in the radial direction. For the integral (B3), we need the scalar product $\mathbf{e}_r\cdot\mathbf{j}=(\hbar/m)R^2(r)Y^2(\Omega)\mathbf{e}_r\cdot\nabla(\phi_r+\phi_\Omega)$. The volume integral (B4) becomes

$$N=\int_0^b R^2(r)r^{D-1}dr\int_\Omega Y^2(\Omega)d\Omega. \tag{B10}$$

For the surface integral (B3), we make the approximation

$$-\partial_t N=\int_A \mathbf{j}\cdot d\mathbf{A}\approx\int_{A'}\mathbf{j}\cdot d\mathbf{A}', \tag{B11}$$

where $\mathbf{A}'$ is the surface of the sphere with radius a, which means that the reflection in the region $b\leq r\leq a$ is neglected and Eq. (B3) becomes

$$-\partial_t N\approx\int_{A'}\mathbf{j}\cdot d\mathbf{A}'=\frac{\hbar}{m}a^{D-1}R^2(a)\phi_r'(a)\int_\Omega Y^2(\Omega)d\Omega. \tag{B12}$$

By inserting Eqs. (B12), (B10), and (B9) into Eq. (B6), we finally obtain the formula

$$\Gamma=\frac{\hbar^2 k}{m}\frac{R^2(a)a^{D-1}}{\int_0^b R^2(r)r^{D-1}dr} \tag{B13}$$

for the decay coefficient of a resonance with the chemical potential μ of the potential $V(r)$ with the finite range a, which is trapped inside the region $0\leq r\leq b$.

The formula (B13) for $D=1$ resembles Eq. (22). In contrast to formula (B13), the wave number k_{sk} in Eq. (22) is complex and the integration extends over the whole region $r\leq a$. Thus Eq. (B13) can be regarded as an approximation to Eq. (22) [respectively to its generalization to higher dimensions (see [24])].

In the *two-dimensional case,* the ansatz (B8) is only an approximation. As promised above, we discuss this in more detail now by inserting the ansatz

$$\psi(r)=R(r)\exp[i\phi_r(r)] \tag{B14}$$

with real functions $R(r)$ and $\phi(r)$ into the radial part

$$\frac{\partial^2\psi(r)}{\partial r^2}+\frac{1}{r}\frac{\partial\psi(r)}{\partial r}+\frac{2m\mu}{\hbar^2}\psi(r)=0 \tag{B15}$$

of the two-dimensional Schrödinger equation. Separating real and imaginary parts, we arrive at

$$\frac{R''(r)}{R(r)} + \frac{R'(r)}{rR(r)} - \phi_r'^2(r) + \frac{2m\mu}{\hbar^2} = 0, \tag{B16}$$

$$\left(\frac{2R'(r)}{R(r)} + \frac{1}{r}\right)\phi_r'(r) + \phi_r''(r) = 0. \tag{B17}$$

The choice $R(r)=C/\sqrt{r}$ and $\phi_r(r)=kr+\phi_0$ with real constants C, k, and ϕ_0 solves the lower equation. The remaining equation yields $k^2=2m\mu/\hbar^2+r^{-2}/4$. Thus Eq. (B15) is approximately solved by $\psi(r)=C/\sqrt{r}\exp(ikr+\phi_0)$ with $k=\sqrt{2m\mu}/\hbar$ if $r^2 \gg \hbar^2/(8m\mu)$ so that the length a in Eq. (B8) must be chosen accordingly.

Applicability to the NLSE. In the case of the NLSE (2), the ansatz (B7) and (B8) and thus formula (B13) are still valid in many cases where the wave equation can still be separated into a radial part and an angular part.

For $D=1$, inserting the ansatz (B7) and (B8) into the nonlinear term in Eq. (2) leads to $g|\psi(\mathbf{x})|^2=gR^2(r)Y^2(\Omega)=gR^2(r)$ since $Y(\Omega)=\pm 1$. This means that the nonlinear term only modifies the radial part of the wave equation, whereas the angular part is not affected. For $r\geq a$, $g|\psi(\mathbf{x})|^2=gR^2(a)$ is a constant term that only causes a shift in the chemical potential. If $gR^2(a)<\mathrm{Re}(\mu)$, this can be accounted for by replacing $\mu \to \mu - gR^2(a)$ so that the wave vector is now given by $k=\mathrm{Re}\{\sqrt{2m[\mu-gR^2(a)]}/\hbar\}$.

If $D=2$, we also have $|Y(\Omega)|=1$, so that the wave function can still be separated into a radial part and an angular part in analogy to the one-dimensional case. For $r\geq a$, $g|\psi(\mathbf{x})|^2=gR^2(a)a/r$. Thus for $|g|R^2(a)\ll|\mu|$ we can neglect the influence of the nonlinear term in the region $r\geq a$ and the ansatz (B8) is still valid.

For $D=3$, we have $|Y(\Omega)|\neq 1$ in general so that the wave equation can no longer be separated into a radial part and an angular part and thus the ansatz (B7) and (B8) fails. However, for the special case of s-wave solutions, $|Y(\Omega)|=1$ still holds and in analogy to the case $D=2$, formula (B13) is approximately valid if $|g|R^2(a)\ll|\mu|$.

[1] R. Folman, P. Krüger, D. Cassettari, B. Hessmo, T. Maier, and J. Schmiedmayer, Phys. Rev. Lett. **84**, 4749 (2000).

[2] W. Hänsel, P. Hommelhoff, T. W. Hänsch, and J. Reichel, Nature (London) **413**, 498 (2001).

[3] H. Ott, J. Fortagh, G. Schlotterbeck, A. Grossmann, and C. Zimmermann, Phys. Rev. Lett. **87**, 230401 (2001).

[4] E. Andersson, T. Calarco, R. Folman, M. Andersson, B. Hessmo, and J. Schmiedmayer, Phys. Rev. Lett. **88**, 100401 (2002).

[5] C. D. J. Sinclair, E. A. Curtis, I. L. Garcia, J. A. Retter, B. V. Hall, S. Eriksson, B. E. Sauer, and E. A. Hinds, Phys. Rev. A **72**, 031603 (2005).

[6] A. E. Leanhardt, A. P. Chikkatur, D. Kielpinski, Y. Shin, T. L. Gustavson, W. Ketterle, and D. E. Pritchard, Phys. Rev. Lett. **89**, 040401 (2002).

[7] M. Singh, M. Volk, A. Akulshin, A. Sidorov, R. McLean, and P. Hannaford, J. Phys. B **41**, 065301 (2008).

[8] C. J. Vale, B. Upcroft, M. J. Davis, N. R. Heckenberg, and H. Rubinsztein-Dunlop, J. Phys. B **37**, 2959 (2004).

[9] J. Bravo-Abad, M. Ibanescu, J. D. Joannopoulos, and M. Soljacic, Phys. Rev. A **74**, 053619 (2006).

[10] W. Guerin, J.-F. Riou, J. P. Gaebler, V. Josse, P. Bouyer, and A. Aspect, Phys. Rev. Lett. **97**, 200402 (2006).

[11] L. Pitaevskii and S. Stringari, *Bose-Einstein Condensation* (Oxford University Press, Oxford, 2003).

[12] A. S. Parkins and D. F. Walls, Phys. Rep. **303**, 1 (1998).

[13] F. Dalfovo, S. Giorgini, L. Pitaevskii, and S. Stringari, Rev. Mod. Phys. **71**, 463 (1999).

[14] A. J. Leggett, Rev. Mod. Phys. **73**, 307 (2001).

[15] R. K. Dodd, J. C. Eilbeck, J. D. Gibbon, and H. C. Morris, *Solitons and Nonlinear Wave Equations* (Academic, London, 1982).

[16] T. Paul, K. Richter, and P. Schlagheck, Phys. Rev. Lett. **94**, 020404 (2005).

[17] T. Paul, P. Leboeuf, N. Pavloff, K. Richter, and P. Schlagheck, Phys. Rev. A **72**, 063621 (2005).

[18] D. Witthaut, S. Mossmann, and H. J. Korsch, J. Phys. A **38**, 1777 (2005).

[19] K. Rapedius, D. Witthaut, and H. J. Korsch, Phys. Rev. A **73**, 033608 (2006).

[20] P. Leboeuf and N. Pavloff, Phys. Rev. A **64**, 033602 (2001).

[21] D. Witthaut, K. Rapedius, and H. J. Korsch, arXiv:cond-mat/0506645.

[22] L. D. Carr, K. W. Mahmud, and W. P. Reinhardt, Phys. Rev. A **64**, 033603 (2001).

[23] T. Paul, M. Hartung, K. Richter, and P. Schlagheck, Phys. Rev. A **76**, 063605 (2007).

[24] A. J. F. Siegert, Phys. Rev. **56**, 750 (1939).

[25] P. Schlagheck, "Tunneling in the presence of chaos and interactions," Habilitation thesis, Universität Regensburg, 2006.

[26] R. E. Mickens, *An Introduction to Nonlinear Oscillations* (Cambridge University Press, Cambridge, 1981).

[27] P. Schlagheck and T. Paul, Phys. Rev. A **73**, 023619 (2006).

[28] P. Schlagheck and S. Wimberger, Appl. Phys. B: Lasers Opt. **86**, 385 (2007).

[29] N. Moiseyev, Phys. Rep. **302**, 212 (1998).

[30] N. Moiseyev, L. D. Carr, B. A. Malomed, and Y. B. Band, J. Phys. B **37**, L193 (2004).

[31] S. Wimberger, P. Schlagheck, and R. Mannella, J. Phys. B **39**, 729 (2006).

[32] S. A. Gredeskul and Y. S. Kivshar, Phys. Rep. **216**, 1 (1992).

[33] T. Volz, S. Dürr, S. Ernst, A. Marte, and G. Rempe, Phys. Rev. A **68**, 010702 (2003)

[34] M. Abramowitz and I. A. Stegun, *Handbook of Mathematical Functions* (Dover, New York, 1972).

[35] H. Cartarius, J. Main, and G. Wunner, Phys. Rev. A **77**, 013618 (2008).